



## Analysis of submicron-sized niflumic acid crystals prepared by electrospray crystallization

Rita Ambrus<sup>a</sup>, Norbert Radacsi<sup>b</sup>, Tímea Szunyogh<sup>a</sup>, Antoine E.D.M. van der Heijden<sup>b,c</sup>,  
Joop H. ter Horst<sup>b</sup>, Piroska Szabó-Révész<sup>a,\*</sup>

<sup>a</sup> Department of Pharmaceutical Technology, University of Szeged, Eötvös 6, H-6720 Szeged, Hungary

<sup>b</sup> Process & Energy Laboratory, Delft University of Technology, Leeghwaterstraat 44, 2628 CA Delft, Netherlands

<sup>c</sup> Technical Sciences, TNO, 2280 AA Rijswijk, Netherlands

### ARTICLE INFO

#### Article history:

Received 26 June 2012

Received in revised form 31 October 2012

Accepted 2 December 2012

Available online xxx

#### Keywords:

Nanoparticles

Electrospray crystallization

Anti-solvent crystallization

Solvent evaporation

Niflumic acid

Physico-chemical analysis

### ABSTRACT

Interest in submicron-sized drug particles has emerged from both laboratory and industrial perspectives in the last decade. Production of crystals in the nano size scale offers a novel way to particles for drug formulation solving formulation problems of drugs with low solubility in class II of the Biopharmaceutical Classification System. In this work niflumic acid nanoparticles with a size range of 200–800 nm were produced by the novel crystallization method, electrospray crystallization. Their properties were compared to those from evaporative and anti-solvent crystallizations, using the same organic solvent, acetone. There is a remarkable difference in the product crystal size depending on the applied methods. The size and morphology were analyzed by scanning electron microscopy and laser diffraction. The structure of the samples was investigated using differential scanning calorimetry, Fourier-transformed infrared spectroscopy and X-ray powder diffraction. The particles produced using electrospray crystallization process were probably changing from amorphous to crystalline state after the procedure.

© 2012 Elsevier B.V. All rights reserved.

### 1. Introduction

Niflumic acid (NIF) is an important anti-inflammatory drug and has a weak analgesic effect. It is primarily used to treat different forms of rheumatism, like rheumatoid arthritis or arthrosis, and to cure other inflammatory diseases [1]. However, its poor aqueous solubility and dissolution rate are disadvantages [2]. To achieve optimal pharmacodynamic properties such as a rapid onset of the drug effect, fast dissolution is important for this type of drug. In our earlier studies, the aim was to improve the solubility and dissolution rate, via the preparation of ternary systems of NIF, cyclodextrin (CD) and polyvinylpyrrolidone (PVP K-25) in different NIF to CD to PVP ratios by physical mixing, kneading, microwave irradiation and micronization [3–6].

The interest for nano/micron particles in pharmaceutical research has emerged recently, since studies have proven that particle size reduction can influence the mechanisms of drug delivery in many ways [7–14]. The different methods used for particle size reduction can be divided into two main categories: top-down method, where the raw material is subsequently broken down by using milling methods until micro- or nanosized particles are

produced and the bottom-up approach (crystallization procedure), the basic principle of which involving dissolution of the drug in a solvent, followed by addition of the solution to a non-solvent, as a consequence of which the drug precipitates. The nanosuspension engineering processes currently used include precipitation using high-pressure homogenization in water, in mixtures of water and water-miscible liquids, or in non-aqueous media [15–19]. Electrospray crystallization as a novel possibility in bottom-up procedure, has the potential to become an efficient, cost-effective method for the production of submicron-sized organic crystals [20], offering a simple formulation way of pharmaceutical ingredients with beneficial properties [21–23].

In electrospray crystallization a high, constant potential difference is applied to a nozzle, through which a conductive solution is pumped (Fig. 1). If the potential difference is sufficiently high, electrostatic forces overcome the surface tension and a jet of liquid is emitted from the so-called Taylor-cone formed at the nozzle. At some distance from the nozzle, the jet becomes unstable and breaks into droplets, which are accelerated toward the grounded plate by the electric field. Coalescence of the droplets is prevented because of the unipolar charge [21] (which enables production of nano-sized crystals). Upon using a sufficiently volatile solvent such as acetone, solvent evaporation occurs, which increases the specific surface charge density because of the decrease in droplet volume and surface area. As the surface charge density reaches a critical

\* Corresponding author. Tel.: +36 62 545575; fax: +36 62 545571.

E-mail address: [revesz@pharm.u-szeged.hu](mailto:revesz@pharm.u-szeged.hu) (P. Szabó-Révész).

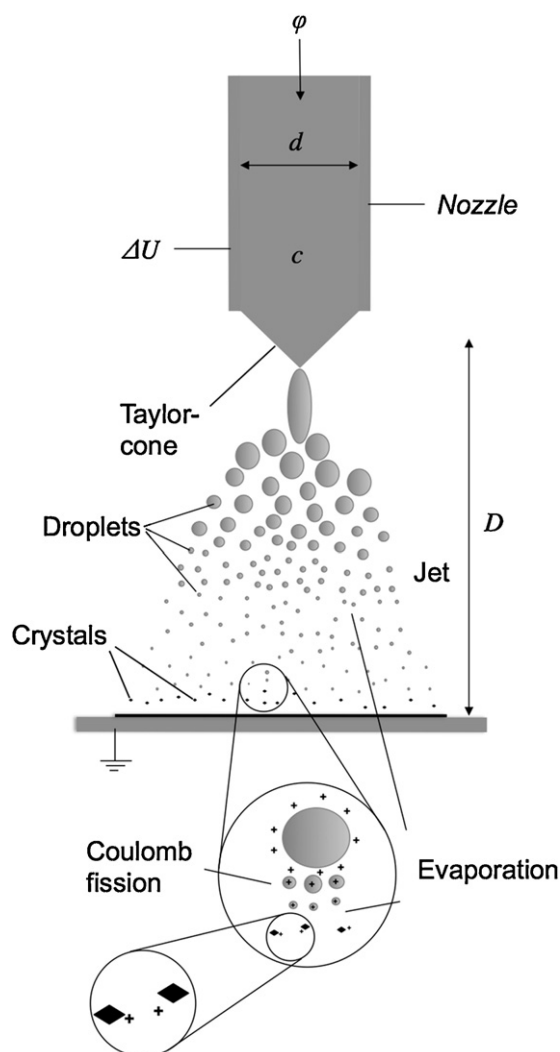


**Fig. 1.** Schematics of the electro spray crystallization process. Using a small nozzle diameter ( $d$ ), a low constant flow rate ( $\phi$ ), relatively low solute concentration ( $c$ ) a jet of highly charged small droplets will be emitted from the cone appearing at the nozzle tip when applying a high enough potential difference ( $\Delta U$ ) at a certain working distance ( $D$ ).

value (Rayleigh-limit) [24] electrostatic forces overcome the surface tension and the droplet disrupts into smaller droplets to reduce the surface charge density by creating more surface area. This disruption process is called Coulomb-fission. At some point during this process of droplet evaporation and disruption, the driving force for crystallization becomes sufficiently large for crystal nucleation and growth to occur. It is assumed that crystallization is confined to the volume of the droplet [25]. Therefore, if the droplets are sufficiently small, typically one crystal per droplet is formed. These charged submicron crystals accumulate at the grounded surface where they lose their surface charge.

It is known that the electro spray crystallization results in NIF particles with significantly improved dissolution rate [26], and this paper is meant to characterize the produced submicron crystals. The goal of this research was to prepare and analyze submicron-sized NIF crystals. Hereby electro spray crystallization is introduced as a potential inexpensive and simple method for the production of such submicron-sized drug crystals and compared to conventional evaporative anti-solvent crystallizations. The effect of three different crystallization methods (electro spray crystallization, anti-solvent crystallization and evaporative crystallization) on

the crystal structure, product and size micrometric properties is investigated and compared with the conventional NIF.

## 2. Materials and methods

### 2.1. Materials

Conventional niflumic acid (NIF) (2-[[3-(trifluoromethyl) phenyl]amino]-3-pyridinecarboxylic acid) with broad crystal size distribution and a mean size of around  $80 \mu\text{m}$  was purchased from G. Richter Pharmaceutical Factory, Budapest, Hungary. For all the crystallization processes the solution was prepared with 99.8% acetone, purchased from Merck.

### 2.2. Methods

#### 2.2.1. Preparation procedure

**2.2.1.1. Electro spray crystallization.** An eight-nozzle electro spray crystallization setup with different NIF concentrations (10, 20 and  $30 \text{ mg ml}^{-1}$ ) was used to produce the submicron-sized NIF. The setup consisted of eight nozzles, a nozzle holder, a grounded stainless steel collector plate, a Meredos TL-EAD peristaltic pump, which provided an equal distribution of the solution flow over the nozzles, and a Wallis  $\pm 10 \text{ kV DC}$  power supply that was used in positive DC mode to provide the potential difference between the tip of the nozzles and the grounded plate. The used nozzles had a length of 25.4 mm and the inner diameter of 0.33 mm. They were purchased from EFD, USA. The product designated in the text as NIF-NANO refers to the sample after 2 weeks storage.

**2.2.1.2. Anti-solvent crystallization (AC).** In this method, a solution of 500 mg of NIF in 5 ml of acetone was added to 25 ml of an aqueous media at room temperature ( $25^\circ\text{C}$ ) that was acting as an anti-solvent (Fig. 2). Due to the anti-solvent effect (acetone is miscible with water, and water acts as an anti-solvent for NIF), the driving force for crystallization was reached rapidly, and a suspension of precipitated crystals was produced in water. This process was carried out by using a T-25 type of Ultra-Turrax disperser simultaneously (IKA, Staufen, Germany) at 24,000 rpm for 10 min, as energy input for size decreasing (the growth of the precipitated crystal could be controlled). This very high stirring rate results in a slight temperature increase (up to  $33^\circ\text{C}$ ) and enhances the evaporation rate of the acetone from the mixture. The product was filtered and dried at room temperature, then investigated immediately. The product is labeled as NIF-AC in the paper.

**2.2.1.3. Preparation of the sample by solvent evaporation (SE).** An amount of 250 mg NIF was dissolved in 5 ml acetone, and then the solvent was evaporated with the help of a cold dryer (HM 3 Dryer,

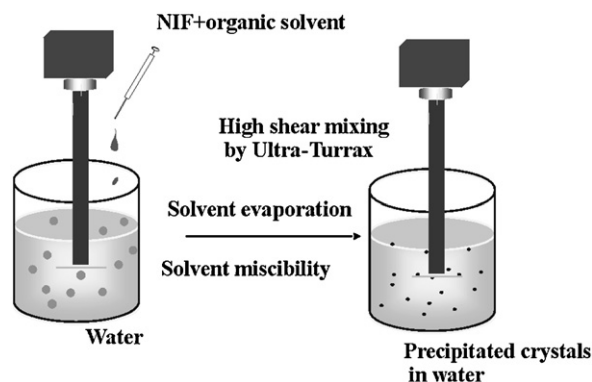


**Fig. 2.** Schematic drawing of the anti-solvent crystallization method.

MH9150201, Siemens, Germany) at 20 °C until all the acetone evaporated. Then the dry powder was pulverized and homogenized manually in a mortar to ensure a narrow crystal size distribution. Then the product was investigated immediately. The NIF produced by evaporative crystallization is labeled in the text as NIF-SE in the paper.

### 2.3. Analysis

#### 2.3.1. Scanning electron microscopy (SEM)

The crystal size and shape were examined by scanning electron microscopy (Hitachi S4700, Hitachi Scientific Ltd., Japan). A sputter coating apparatus (Bio-Rad SC 502, VG Microtech, England) was applied to induce electric conductivity on the surface of the samples. The air pressure was 1.3–13.0 mPa. Samples were fixed onto a metallic stub with double-sided conductive tape (diameter 12 mm, Oxon, Oxford Instruments, UK). Images were taken in secondary electron image mode at 10 kV acceleration voltage. The particle diameter distributions were obtained by analyzing several SEM images with the ImageJ software environment [27]. Over 150 individual particle measurements were made using at least five different images in order to determine the particle size distribution.

#### 2.3.2. Particle size analysis

The particle size distribution of the conventional NIF was measured by a laser diffractometer (Mastersizer S, Malvern Instruments Ltd., Worcestershire, UK) with the following parameters: 300RF lens, small volume dispersion unit rotated at 2000 rpm, 1.510 refractive index for dispersed particles, and 1.330 refractive index for the dispersion medium.

#### 2.3.3. Differential scanning calorimetry (DSC)

DSC was employed to investigate the crystallization behavior and the melting behavior of the conventional and submicron-sized NIF. The DSC measurements were made with a Mettler Toledo DSC 821<sup>e</sup> thermal analysis system with the STAR<sup>e</sup> thermal analysis program V9.1 (Mettler Inc., Schwerzenbach, Switzerland). Approximately 2–5 mg of product was examined in the temperature range between 25 °C and 300 °C. The heating rate was 5 °C min<sup>-1</sup>. Argon was used as a carrier gas, at a flow rate of 101 h<sup>-1</sup> during the DSC investigation.

The crystallinity index of the different NIF samples was calculated from the heats of fusion: the ratio between the normalized enthalpy of the NIF samples and the normalized enthalpy of the conventional NIF indicates the product crystallinity [28].

#### 2.3.4. X-ray powder diffraction (XRPD)

XRPD was carried out in order to determine the crystalline form and crystallinity of the produced materials. Samples were measured with a Bruker D8 Advance diffractometer (Bruker AXS GmbH, Karlsruhe, Germany). Data collection was carried out at room temperature using monochromatic Cu K $\alpha$ 1 radiation ( $\lambda = 0.154060$  nm) in the  $2\theta$  region between 3° and 50°. For measurements directly after electrospay crystallization, about 10 milligrams of sample was directly deposited on a zero background holder (Si single crystal <510> wafer) and placed into the XRD directly after production. The recording of the pattern was relatively fast, it lasted 180 s. Diffraction patterns were recorded from 15 min till 20 h after production at different time intervals.

#### 2.3.5. Fourier transform infrared spectroscopy (FT-IR)

FT-IR spectroscopy was used to investigate the chemical stability of the drug. FT-IR spectra were measured on an AVATAR 330 FT-IR apparatus (Thermo Nicolet, USA), in the interval 400–4000 cm<sup>-1</sup>, at 4 cm<sup>-1</sup> optical resolution. Standard KBr pellets

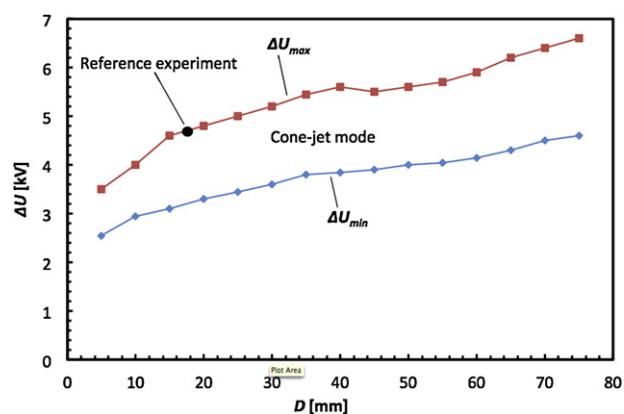


Fig. 3. The relation between working distance ( $D$ ) and potential difference ( $\Delta U$ ).

were prepared from 150 mg of KBr pressed with 10 ton and samples containing 0.5 mg of NIF were used.

## 3. Results and discussion

### 3.1. Electrospay crystallization process parameters

The electrospay crystallization process parameters were determined for the production of the desired submicron product. Three process parameters were identified to have a major effect on the product: initial solute concentration ( $c$ ), potential difference ( $\Delta U$ ) and nozzle diameter ( $d$ ). The flow rate ( $\varphi$ ) could not be investigated, since the operation window of the flow rate was too low, and changes in flow rate resulted in instable jet. The working distance ( $D$ ) strongly depends on the applied potential difference: larger distances demand higher potential difference. Fig. 3 shows the relationship between working distance  $D$  and potential difference  $\Delta U$ .

When higher initial concentrations were used, the average crystal size increased: the same droplet with a higher concentration contains more solute that can crystallize, resulting in larger crystals (Fig. 4). The crystal shape also depends on the initial concentration. At higher concentrations, the obtained crystals were more needle-like, while at lower concentrations the crystals had somewhat spherical shape (Fig. 4).

A lower potential difference resulted in agglomeration of crystals. The increase of the nozzle diameter also results in agglomerate

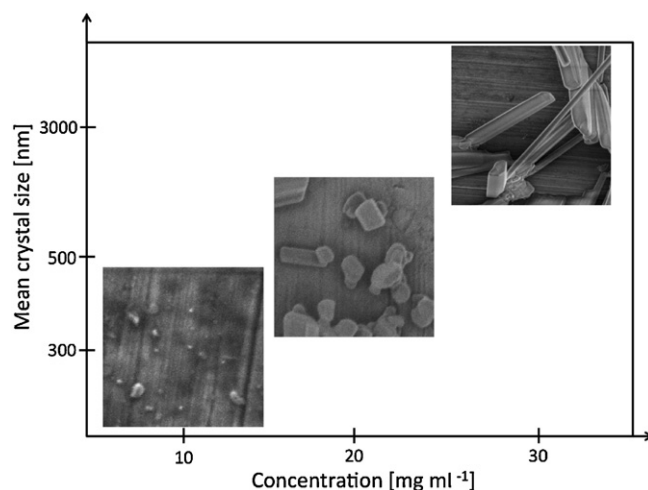
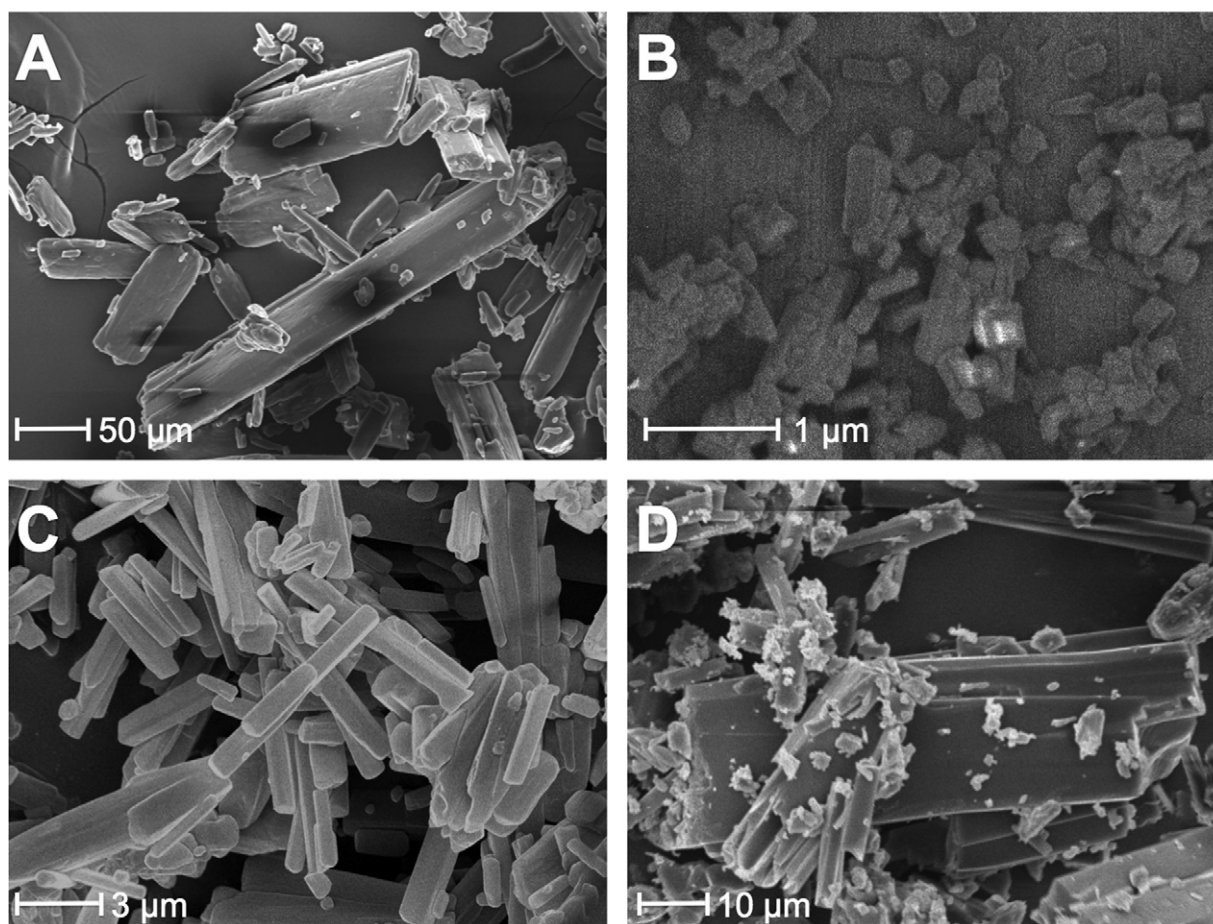


Fig. 4. The relationship between the crystal size and shape and used solution concentration of NIF crystals, produced by electrospay crystallization.



**Fig. 5.** SEM images of (a) conventional NIF, (b) NIF produced by electrospray crystallization (NIF-NANO), (c) NIF produced by anti-solvent crystallization (NIF-AC) and (d) NIF produced by solvent evaporation (NIF-SE).

formation [26]. A lower potential difference or larger nozzle diameter results in a lower charge density at the Taylor-cone and therefore at the droplet surface. At a lower surface charge density Coulomb-fission is occurring later or is absent and crystallization might occur in larger droplets, resulting in agglomerated crystals.

The optimal process parameters for producing submicron-sized NIF crystals (NIF-NANO) with a compact shape without agglomeration were found to be: solution concentration of  $20 \text{ mg ml}^{-1}$ , a potential difference of  $+4.7 \text{ kV}$ , a nozzle diameter of  $0.33 \text{ mm}$ , a working distance of  $17 \text{ mm}$  and a flow rate of  $1.8 \text{ ml h}^{-1}$ . With these parameters somewhat prismatic shape NIF crystals with a mean size of around  $500 \text{ nm}$  were produced. The production rate under these conditions was  $150 \text{ mg h}^{-1}$ .

### 3.2. Product size and shape

The conventional NIF crystals had a smooth surface with prismatic shape with around  $80 \mu\text{m}$  mean size and a broad crystal size distribution (Fig. 5A). This shape was also seen for the NIF-SE crystals (Fig. 5D). The crystal shape of NIF-SE was prismatic as well, and its size distribution was very broad with an estimate mean size of around  $46 \mu\text{m}$ , probably due to the applied homogenization by manual pulverization. By using the anti-solvent crystallization method (NIF-AC), needle-like NIF crystals in the size of around  $10 \mu\text{m}$  were produced (Fig. 5C). This crystallization method combined with high shear mixing is an effective procedure for the particle size decreasing toward the micron range. The electrospray crystallization procedure caused the most remarkable alterations

from all the used crystallization methods. After the procedure, somewhat spherical shaped NIF particles were found with a mean size of  $500 \text{ nm}$  (Fig. 5B). These submicron particles are clustered into aggregates up to  $20 \mu\text{m}$  in size, possibly due to the strong cohesive interactions between the hydrophobic crystal surfaces with the increased specific surface area.

Table 1 presents the mean particle size of NIF determined using a SEM images analysis. It can be seen that the solvent evaporation with pulverization of the crystals (NIF-SE) decreased the crystal size to nearly half that of the conventional NIF size ( $80 \mu\text{m}$ ) determined. The product produced by the anti-solvent crystallization process (AC) resulted in crystals around  $7 \mu\text{m}$ . Electrospray crystallization resulted in nano-sized particles, around  $500 \text{ nm}$ . It seems that the increase in supersaturation in the anti-solvent crystallization process is not enough to obtain submicron crystals. Also the crystallization volume should be decreased, as in electrospray crystallization the main reason of size decreasing is that micron-sized droplets are created in the process, and crystallization commences in the small, confined volume offered by the droplets.

**Table 1**  
The calculated mean crystal size of the conventional NIF and the produced crystals.

Sample	Mean size ( $\mu\text{m}$ ) $\pm$ SD
NIF	$80 \pm 22.6$
NIF-NANO	$0.5 \pm 0.2$
NIF-AC	$7.4 \pm 3.9$
NIF-SE	$46.2 \pm 26.0$

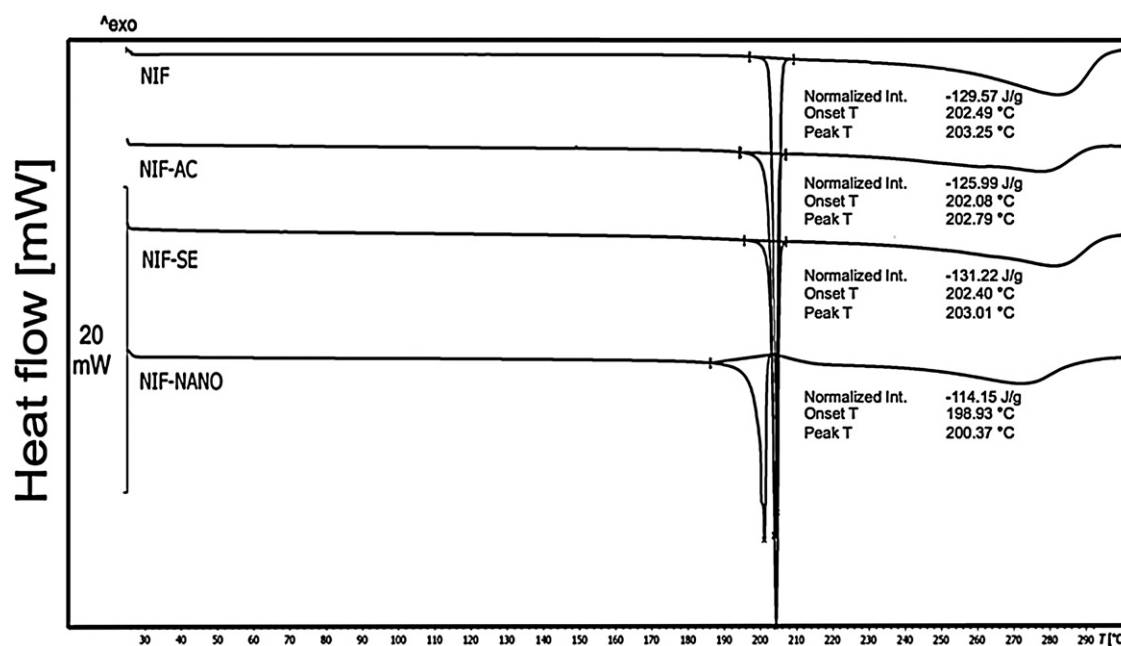


Fig. 6. DSC curve of the conventional NIF compared with the recrystallized NIF obtained from the solvent evaporation (NIF-SE), the recrystallized NIF obtained from the antisolvent crystallization (NIF-AC) and the submicron-sized NIF from electro spray crystallization (NIF-NANO).

### 3.3. Structural analysis (DSC, XRPD and FT-IR)

The presence of amorphous fraction could be expected by spraying crystallization techniques, since the driving forces for crystallization are high [29,30]. The presence of amorphous fraction has an effect on the stability of the samples as well. Due to the rapid evaporation of the solvent in electro spray crystallization, the crystal structure might not build up completely (kinetically formed more slowly) during the crystallization process [31]. Thus structural characterizations were performed to check the crystalline state of the produced NIF crystals.

#### 3.3.1. Differential scanning calorimetry

DSC was used to measure the melting point ( $T$ ) and the heat of melting. The onset  $T$  of the conventional NIF at 202.49 °C reflected its melting point (Fig. 6). The NIF-AC and NIF-SE samples presented similar DSC curves with a melting point at around 202 °C. The submicron-sized NIF (NIF-NANO) had a well detectable melting point at a lower temperature (198.93 °C). The lower melting point and broader peak of the submicron-sized drug can be explained by the relatively large proportion of surface molecules compared to the bulk. The vibrational and positional enthalpy and entropy of surface molecules of submicron-sized materials are different from that of molecules inside the bulk of the crystals, which can alter physical properties, including thermal properties [32]. One way to test the crystallinity of the samples is to determine the normalized heat of melting, since there is a relation between the heat of melting and the crystalline fraction of the sample [28].

The crystallinity index of NIF was calculated from the normalized heat of melting of the samples (Table 2). The conventional NIF sample was assumed to have 100% crystallinity. The sample produced by solvent evaporation (NIF-SE) showed higher heat of melting than the conventional NIF, probably due to the pulverization impact during the preparation procedure. The sample from the anti-solvent crystallization method (NIF-AC) showed 97% crystallinity. The electro spray crystallization product (NIF-NANO) showed the lowest crystallinity from all the produced samples, 88% of the material was measured to be crystalline, which implies that 12% of the sample is amorphous. The crystallinity index was also

Table 2

The crystallinity index (CI) of the samples according to the DSC measurements.

Sample	Normalized integral ( $J g^{-1}$ )	CI (%)
NIF	129.57 ± 0.23	100
NIF-SE	131.22 ± 0.45	100
NIF-AC	125.99 ± 0.36	97
NIF-NANO (2 weeks after preparation)	114.15 ± 0.82	88
Electrosprayed NIF (15 min after the procedure)	105.32 ± 0.39	81

calculated for a sample that was measured 15 min after the production by the electro spray crystallization process. Its crystallinity index was 81%, 7% less than the electro sprayed sample after 2 weeks (NIF-NANO). This shows that a part of NIF changed from amorphous phase to crystalline phase during the storage.

To summarize the DSC results, the reason of melting depression is a part of amorphous state and particles size decrease of NIF.

#### 3.3.2. X-ray powder diffraction

XRPD analysis was used to examine the crystal structure and it was also used to assess the crystallinity of the products. The characteristic intensity values of the NIF can be found at 8.2, 12.9, 16.2, 23.2, 25.7  $2\theta$  values. All the produced samples showed peaks at the same positions as the conventional NIF, but their intensity was lower (Fig. 7). When the three produced samples are compared with each other, it can be seen that the NIF-SE sample has more intense peaks, than the NIF-AC or NIF-NANO samples, indicating that the NIF-SE sample has higher crystallinity than the other two products. The peak intensity of the NIF-AC sample is in between the NIF-SE and the NIF-NANO samples. From the three produced materials, the NIF-NANO sample presents the lowest peak intensities, indicating the lowest crystalline fraction from the measured products. Since in general the evaporative crystallization results in highly crystalline product, it was assumed that the NIF-AC and NIF-NANO samples are partially amorphous. The particle size decrease of the NIF-AC and NIF-NANO samples also can be the reason for the measured lower intensities in the XRPD patterns.

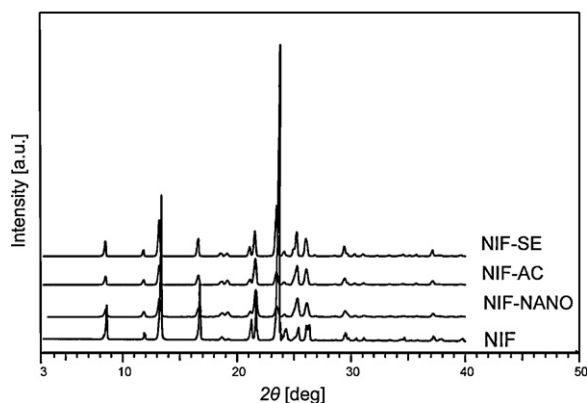


**Fig. 7.** XRPD patterns of the NIF samples produced by solvent evaporation (NIF-SE), anti-solvent crystallization (NIF-AC) and electrospray crystallization (NIF-NANO), compared with the conventional NIF (NIF).

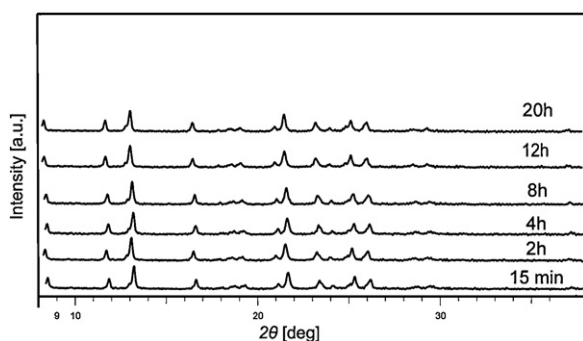


**Fig. 8.** XRPD pattern of the produced NIF-NANO sample till 20 h after the procedure.

To investigate a possible transition between amorphous and crystalline state of the NIF-NANO sample, diffraction patterns of the sample was recorded directly after spraying for 20 h. The crystallinity did not change in the first 20 h (Fig. 8). Since the XRPD pattern of the NIF-NANO sample (which means the nanoparticles 2 weeks after electrospray crystallization) showed higher intensities than can be seen on the 20 h diffraction pattern, probably the crystallinity increased further in the following two weeks.

### 3.3.3. FT-IR analysis

IR spectroscopy was used to study the chemical stability of the NIF samples. The IR spectrum of NIF displays strong

absorption at  $1607\text{ cm}^{-1}$  that is due to the characteristic  $\nu_{\text{as}}(\text{COO})$  and  $\nu_{\text{s}}(\text{COO})$  stretching modes of carboxyl groups. A middle-strong peak at  $3163\text{ cm}^{-1}$  can be ascribed to the N–H vibration of imine [33,34], and the strong absorption peak at  $1523\text{ cm}^{-1}$  is owing to the framework vibration of the phenyl and pyridine rings. The FT-IR spectra (Fig. 9) of NIF-SE and NIF-NANO did not present differences compared with NIF. New bonds were not developed and old bonds did not disappear. According to the FT-IR analysis no chemical change in the structure was detected, which means that the produced samples did not show polymorphic transition or chemical decomposition. This implies that the produced NIF-NANO crystals are chemically stable before and after the procedure.

## 4. Conclusions

This study has shown that electrospray crystallization as a non-conventional method can be used to formulate submicron-sized NIF crystals with a mean size of around 500 nm. Careful selection of preparation parameters is critical to achieve the suitable size and shape. Lower initial solution concentrations lead to compact, somewhat spherical crystal shape, while higher concentrations result in needle-like crystals. The crystallization procedure was compared to two conventional crystallization methods, evaporative and anti-solvent crystallization, where macro- and micro-sized crystals were prepared. XRPD measurements of the immediately produced NIF crystals showed that by evaporative and anti-solvent crystallization the products were highly crystalline right after production and also after 2 weeks. However the electrosprayed product was partly amorphous right after the production, and only 81% of the sample was crystalline. The crystallinity of the electrosprayed sample has increased during storage, according to the DSC results the two-week-old electrosprayed NIF samples were 88% crystalline. According to the FT-IR measurements the NIF crystals were chemically stable before and after the procedure.

## Acknowledgement

The publication/presentation is supported by the European Union and cofunded by the European Social Fund. Project number: TÁMOP-4.2.2/B-10/1-2010-2012.

Project title: "Broadening the knowledge base and supporting the long term professional sustainability of the Research University Center of Excellence at the University of Szeged by ensuring the rising generation of excellent scientists."

## References

- [1] The Merck Index, 14th ed., Merck & Co. Inc., Rahway, NJ, 2012 (<http://themerckindex.chemfinder.com>).
- [2] Martindale, The Extra Pharmacopoeia, 37th ed., The Royal Pharm. Society, London, 2011, pp 234–282.
- [3] R. Ambrus, Z. Aigner, C. Dehelean, C. Soica, P. Szabó-Révész, Physico-chemical studies on solid dispersions of niflumic acid prepared with PVP, *Rev. Chim.* 58 (2007) 60–64.
- [4] R. Ambrus, Z. Aigner, C. Soica, C. Peev, P. Szabó-Révész, Amorphisation of niflumic acid with polyvinylpyrrolidone prepared solid dispersion to reach rapid drug release, *Rev. Chim.* 58 (2007) 206–209.
- [5] M. Kata, R. Ambrus, Z. Aigner, Preparation and investigation of inclusion complexes containing niflumic acid and cyclodextrins, *J. Inc. Phenom.* 44 (2002) 123–126.
- [6] T. Szunyogh, R. Ambrus, P. Szabó-Révész, Importance of particle size decrease in the preformulation, *Acta Pharm. Hung.* 81 (2011) 29–36.
- [7] J. Kanzer, S. Hupfeld, T. Vasskog, I. Tho, P. Hölig, M. Mägerlein, G. Fricker, M. Brandl, In situ formation of nanoparticles upon dispersion of melt extrudate formulations in aqueous medium assessed by asymmetrical flow field-flow fractionation, *J. Pharm. Biomed. Anal.* 53 (2010) 359–365.
- [8] J. Zhang, H. Lv, K. Jiang, Y. Gao, Enhanced bioavailability after oral and pulmonary administration of baicalein nanocrystal, *Int. J. Pharm.* 420 (2011) 180–188.
- [9] T.W. Prow, J.E. Grice, L.L. Lin, R. Faye, M. Butler, W. Becker, E.M.T. Wurm, C. Yoong, T.A. Robertson, H.P. Soyer, M.S. Roberts, Nanoparticles

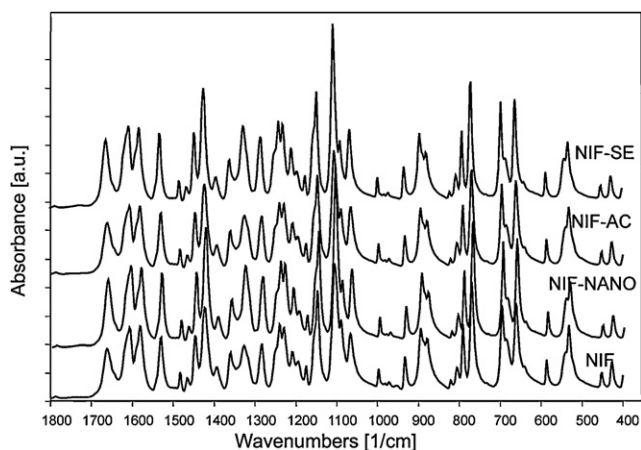


**Fig. 9.** FT-IR spectra of conventional NIF, the electro sprayed NIF-NANO, NIF-AC by anti-solvent crystallization and NIF-SE by solvent evaporation methods.

- and microparticles for skin drug delivery, *Adv. Drug Deliv. Rev.* 63 (2011) 470–491.
- [10] H. Chen, X. Kou, Z. Yang, W. Ni, J. Wang, Shape- and size-dependent refractive index sensitivity of gold nanoparticles, *Langmuir* 24 (2008) 5233–5237.
- [11] D. Missirlis, N. Tirelli, J.A. Hubbel, Amphiphilic hydrogel nanoparticles preparation characterization and preliminary assessment as new colloidal drug carriers, *Langmuir* 21 (2005) 2605–2613.
- [12] J.-W. Kim, M.-S. Shin, J.-K. Kim, H.-S. Kim, K.-K. Koo, Evaporation crystallization of RDX by ultrasonic spray, *Ind. Eng. Chem. Res.* 50 (2011) 12186–12193.
- [13] R. Ambrus, P. Kocbek, J. Kristl, R. Sibanc, R. Rajkó, P. Szabó-Révész, Investigation of preparation parameters to improve the dissolution rate of poorly soluble meloxicam, *Int. J. Pharm.* 318 (2) (2009) 153–159.
- [14] V.A. Saharan, V. Kukkar, M. Kataria, M. Gera, P.M. Choudhury, Dissolution enhancement of drugs. Part I: technologies and effect of carriers, *Int. J. Health Res.* 2 (2009) 107–124.
- [15] G.G. Liversidge, P. Conzentino, Drug particle size reduction for decreasing gastric irritancy and enhancing absorption of naproxen in rats, *Int. J. Pharm.* 125 (1995) 309–313.
- [16] P. Liu, X. Rong, J. Laru, B. von Veen, J. Kiesvaara, J. Hiruonen, T. Laaksonen, L. Peltonen, Nanosuspensions of poorly soluble drugs: preparation and development by wet milling, *Int. J. Pharm.* 411 (2011) 215–222.
- [17] R.H. Müller, A. Akkar, Drug nanocrystals of poorly soluble drugs, *Encyclop. Nanosci. Nanotechnol.* 2 (2004) 627–638.
- [18] P. Kocbek, S. Baumgartner, J. Kristl, Preparation and evaluation of nanosuspension for enhancing the dissolution of poorly soluble drugs, *Int. J. Pharm.* 312 (2006) 179–186.
- [19] T. Yasuji, H. Takeuchi, Y. Kawashima, Particle design of poorly water-soluble substances using supercritical fluid technologies, *Adv. Drug. Dev. Rev.* 60 (2008) 388–398.
- [20] N. Radacsi, A.I. Stankiewicz, Y.L.M. Creighton, A.E.D.M. van der Heijden, J.H. ter Horst, Electro spray crystallization for high-quality submicron-sized crystals, *Chem. Eng. Technol.* 34 (2011) 624–630.
- [21] C.U. Yurteri, R.P.A. Hartman, J.C.M. Marijnissen, Producing pharmaceutical particles via electro spraying with an emphasis on nano and nano structure particles – a review, *KONA Powder Particle J.* 28 (2010) 91–115.
- [22] A. Jaworek, Micro- and nanoparticle production by electro spraying, *Powder Technol.* 176 (2007) 18–35.
- [23] B. Almería, W. Deng, T.M. Fahmy, A. Gomez, Controlling the morphology of electro spray-generated PLGA microparticles for drug delivery, *J. Colloid Interf. Sci.* 343 (2010) 125–133.
- [24] L. Rayleigh, Comparison of methods for the determination of resistances in absolute measure, *Phil. Mag.* 14 (1882) 184–186.
- [25] E. Revalor, Z. Hammadi, J.P. Astier, R. Grossier, E. Garcia, C. Hoff, K. Furuta, T. Okutsu, R. Morin, S. Veessler, Usual and unusual crystallization from solution, *J. Cryst. Growth* 312 (2010) 939–946.
- [26] N. Radacsi, R. Ambrus, T. Szunyogh, P. Szabó-Révész, A.I. Stankiewicz, A.E.D.M. van der Heijden, J.H. ter Horst, Electro spray crystallization for nano-sized pharmaceuticals with improved properties, *Cryst. Growth Des.* 12 (2012) 3514–3520.
- [27] M.D. Abramoff, P.J. Magelhaes, S.J. Ram, Image processing with image, *J. Biophoton. Int.* 11 (2004) 36–42.
- [28] M. Wagner, Thermal analysis in practice, in: DSC evaluations, Mettler Toledo, Schwerzenbach, 2009, pp. 90–141.
- [29] M.J. Arias-Blanco, J.R. Moyano, J.I. Perez-Martinez, J.M. Gines, Study of the inclusion of gliclazide in  $\alpha$ -cyclodextrin, *J. Pharm. Biomed. Anal.* 18 (1998) 275–279.
- [30] H.A. Crisp, J.C. Clayton, L.G. Elliott, E.M. Wilson, Preparation of a highly pure substantially amorphous form of cefuroxime axetil, U.S. Patent 4,820,1833, (1989).
- [31] S. Nakayama, T. Watanabe, M. Senna, Rapid amorphization of molecular crystals by absorption of solvent molecules in the presence of hydrophilic matrices, *J. Alloy. Compd.* 483 (2009) 217–221.
- [32] G.C. Yang, F.D. Nie, J.S. Li, Preparation and characterization of nano-NTO explosive, *J. Energ. Mater.* 25 (2007) 35–47.
- [33] K. Takács-Novák, A. Avdeef, K.J. Box, B. Podányi, Gy Szász, Determination of protonation macro- and microconstants and octanol/water partition coefficient of antiinflammatory drug niflumic acid, *J. Pharm. Biomed. Anal.* 12 (1994) 1369–1377.
- [34] H.M.K. Murthy, M. Vijayan, 2[[3-(Trifluoromethyl)phenyl]amino]-3-pyridinecarboxylic acid (niflumic acid), *Acta Crystallogr.* 35 (1979) 262–263.